PYR/PYL/RCAR Abscisic Acid Receptors Regulate K^+ and Cl^- Channels through Reactive Oxygen Species-Mediated Activation of Ca^{2+} Channels at the Plasma Membrane of Intact Arabidopsis Guard Cells[1][W][OPEN]

Yizhou Wang[2], Zhong-Hua Chen[2], Ben Zhang, Adrian Hills, and Michael R. Blatt*

Laboratory of Plant Physiology and Biophysics, University of Glasgow, Glasgow G12 8QQ, United Kingdom (Y.W., Z.-H.C., B.Z., A.H., M.R.B.); and School of Natural Sciences, University of Western Sydney, Hawkesbury Campus, Richmond, New South Wales 2753, Australia (Z.-H.C.)

The discovery of the START family of abscisic acid (ABA) receptors places these proteins at the front of a protein kinase/phosphatase signal cascade that promotes stomatal closure. The connection of these receptors to Ca^{2+} signals evoked by ABA has proven more difficult to resolve, although it has been implicated by studies of the pyrbactin-insensitive *pyr1/pyl1/pyl2/pyl4* quadruple mutant. One difficulty is that flux through plasma membrane Ca^{2+} channels and Ca^{2+} release from endomembrane stores coordinately elevate cytosolic free Ca^{2+} concentration ($[Ca^{2+}]_i$) in guard cells, and both processes are facilitated by ABA. Here, we describe a method for recording Ca^{2+} channels at the plasma membrane of intact guard cells of Arabidopsis (*Arabidopsis thaliana*). We have used this method to resolve the loss of ABA-evoked Ca^{2+} channel activity at the plasma membrane in the *pyr1/pyl1/pyl2/pyl4* mutant and show the consequent suppression of $[Ca^{2+}]_i$ increases in vivo. The basal activity of Ca^{2+} channels was not affected in the mutant; raising the concentration of Ca^{2+} outside was sufficient to promote Ca^{2+} entry, to inactivate current carried by inward-rectifying K^+ channels and to activate current carried by the anion channels, both of which are sensitive to $[Ca^{2+}]_i$ elevations. However, the ABA-dependent increase in reactive oxygen species (ROS) was impaired. Adding the ROS hydrogen peroxide was sufficient to activate the Ca^{2+} channels and trigger stomatal closure in the mutant. These results offer direct evidence of PYR/PYL/RCAR receptor coupling to the activation by ABA of plasma membrane Ca^{2+} channels through ROS, thus affecting $[Ca^{2+}]_i$ and its regulation of stomatal closure.

Stomatal pores in the epidermis of leaves form the primary route for CO_2 entry for photosynthesis and, at the same time, present a major pathway for foliar water loss by transpiration. The guard cells, which surround the stomatal pore, regulate the aperture of the pore to balance the often conflicting demands for CO_2 and for water conservation. The guard cells open and close the stomatal pore by the uptake and loss, respectively, of osmotic solutes, principally of K^+, Cl^-, and malate (Blatt, 2000; Kim et al., 2010). These transport processes form the visible end of a complex network of interacting regulatory pathways that coordinate plasma membrane and tonoplast and maintain the homeostasis of the guard cell (Chen et al., 2012b; Hills et al., 2012; Wang et al., 2012). A number of well-defined signals, including light, CO_2, drought, and the water stress hormone abscisic acid (ABA), constitute well-defined inputs, each acting on this network to elicit changes in transport, solute content, and stomatal aperture. Over the past three decades, much research has focused on events leading to stomatal closure evoked by ABA. These studies have highlighted both Ca^{2+}-independent and Ca^{2+}-dependent signaling events. Of the latter, elevated free cytosolic Ca^{2+} concentration ($[Ca^{2+}]_i$) plays a critical and early role by inactivating inward-rectifying K^+ channels ($I_{K,in}$) to prevent K^+ uptake and by activating Cl^- (anion) channels (I_{Cl}) at the plasma membrane to depolarize the membrane and engage K^+ efflux through outward-rectifying K^+ channels (Keller et al., 1989; Blatt et al., 1990; McAinsh et al., 1990; Thiel et al., 1992; Lemtiri-Chlieh and MacRobbie 1994). The efflux of K^+ and anions results in a net loss of osmotic content, reducing the turgor and volume of the guard cells to close the stomatal pore.

ABA elevates $[Ca^{2+}]_i$ through the coordination of Ca^{2+} entry at the plasma membrane with Ca^{2+} release from endomembrane stores, a process often described as Ca^{2+}-induced Ca^{2+} release (Grabov and Blatt, 1998; Blatt, 2000). The hormone activates Ca^{2+} channels (I_{Ca}) at the plasma membrane, even in isolated membrane patches (Hamilton et al., 2000), facilitating Ca^{2+} influx (Grabov and Blatt, 1998, 1999; Hamilton et al., 2001). The rise in $[Ca^{2+}]_i$ is linked in part to reactive oxygen species

[1] This work was supported by the Biotechnology and Biological Sciences Research Council (grant nos. BB/H024867/1, BB/F001630/1, and BB/H009817/1 to M.R.B.) and by the Chinese Scholarship Council (Ph.D. studentship to Y.W. and B.Z.).

[2] These authors contributed equally to the article.

* Address correspondence to michael.blatt@glasgow.ac.uk.

The author responsible for distribution of materials integral to the findings presented in this article in accordance with the policy described in the Instructions for Authors (www.plantphysiol.org) is: Michael R. Blatt (michael.blatt@glasgow.ac.uk).

[W] The online version of this article contains Web-only data.

[OPEN] Articles can be viewed online without a subscription.

www.plantphysiol.org/cgi/doi/10.1104/pp.113.219758

(ROS; Pei et al., 2000). The NADPH oxidase mutant *atrbohD/atrbohF* impairs ROS production and I_{Ca} activation in ABA (Kwak et al., 2003). In parallel, cyclic ADP-Ribose production and elevation of nitric oxide enhance the Ca^{2+} sensitivity of endomembrane Ca^{2+} release for $[Ca^{2+}]_i$ elevation (Leckie et al., 1998; Neill et al., 2002; García-Mata and Lamattina, 2003), which is the predominant factor in driving increases in $[Ca^{2+}]_i$. Indeed, simulations of these events (Chen et al., 2012b; Wang et al., 2012) suggest that endomembrane release contributes over 95% of the Ca^{2+} to raise $[Ca^{2+}]_i$.

A large body of evidence also places protein (de-) phosphorylation events within ABA signaling (Armstrong et al., 1995; Li and Assmann, 1996; Grabov et al., 1997; Allen et al., 1999). ABA activates members of the SNF1-related protein (SnRK2) kinase family, notably SnRK2.6/OST1, which promotes the ABA regulation of guard cell transport and is able to phosphorylate both anion and K^+ channels directly (Mustilli et al., 2002; Geiger et al., 2009b; Sato et al., 2009). The 2C-type protein phosphatases ABI1 and ABI2 were identified initially to function upstream of SnRK2 kinases, their activity suppressing ABA action, with subsequent evidence showing that they inactivate SnRK2 kinases by direct dephosphorylation (Geiger et al., 2009b; Umezawa et al., 2009). The discovery of the PYR/PYL/RCAR protein family of ABA receptors, which interact directly with 2C-type protein phosphatases, places these receptor proteins squarely at the front of a protein kinase/phosphatase signal cascade initiated by ABA (Park et al., 2009). Significantly, stomatal movements in the quadruple *pyr1/pyl1/pyl2/pyl4* mutant of Arabidopsis (*Arabidopsis thaliana*) were found to be largely insensitive to ABA, although closure could be evoked if putative downstream signaling elements were engaged, for example by driving $[Ca^{2+}]_i$ with changes in extracellular K^+ and Ca^{2+} concentrations (Nishimura et al., 2010). These observations have been interpreted to indicate that $[Ca^{2+}]_i$ elevation is normally dependent on ABA binding with the PYR/PYL/RCAR receptors. They are consistent, too, with evidence that protein phosphorylation is a prerequisite for Ca^{2+} channel activation (Köhler and Blatt, 2002) and Ca^{2+} release (Sokolovski et al., 2005) in ABA. Lacking, nonetheless, is direct evidence that connects the PYR/PYL/RCAR receptors with $[Ca^{2+}]_i$ elevation in vivo, let alone knowledge that might speak to their association with Ca^{2+} channel activity at the plasma membrane or with other pathways leading to a rise in $[Ca^{2+}]_i$.

Here, we report a strategy for recording I_{Ca} at the plasma membrane of intact guard cells, adapted from methods previously used in voltage-clamp analysis of isolated membrane patches. The strategy enabled parallel measurements with those of $I_{K,in}$ and I_{Cl}, and with Fura2 fluorescence imaging of $[Ca^{2+}]_i$, to explore the response to ABA in wild-type and *pyr1/pyl1/pyl2/pyl4* mutant Arabidopsis. We report that ABA-evoked $[Ca^{2+}]_i$ increases, and the consequent changes in gating of $I_{K,in}$ and I_{Cl}, were suppressed in the *pyr1/pyl1/pyl2/pyl4* mutant and that the effect could be ascribed to a loss in activation of the dominant Ca^{2+} channels at the plasma membrane in

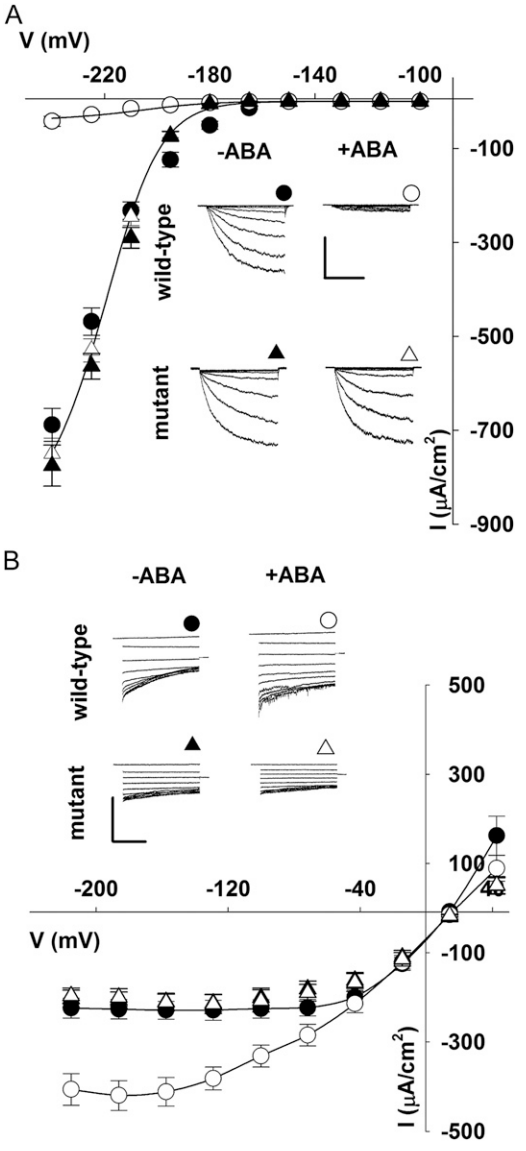

Figure 1. K^+ and Cl^- channel currents of the *pyr1/pyl1/pyl2/pyl4* mutant fail to respond to 20 μM ABA. A, Steady-state current-voltage curves for $I_{K,in}$ recorded in wild-type ($n = 13$) and *pyr1/pyl1/pyl2/pyl4* mutant ($n = 10$) guard cells. Data are means ± SE. Solid curves are fittings to the Boltzmann function (Eq. 2). Parameters are listed in Table I. The inset shows representative $I_{K,in}$ traces during 4-s clamp steps to voltages from −100 to −240 mV cross referenced to the current-voltage curves by symbol. Scale: vertical, 200 μA cm^{-2}; horizontal, 2 s. B, Steady-state current-voltage curves for I_{Cl} recorded in wild-type ($n = 15$) and *pyr1/pyl1/pyl2/pyl4* mutant ($n = 13$) guard cells. Data are means ± SE. Solid curves are empirical fittings to third-order polynomials and are included for clarity. The inset shows representative I_{Cl} traces during 8-s clamp steps to voltages from +40 to −240 mV following 10-s clamp steps at +40 mV. Data are cross referenced to the current-voltage curves by symbol. Scale: vertical, 300 μA cm^{-2}; horizontal, 5 s.

ABA. The *pyr1/pyl1/pyl2/pyl4* mutant was impaired in ROS production, and adding hydrogen peroxide (H_2O_2) was sufficient to recover both Ca^{2+} channel activity and stomatal closing in the mutant. These results demonstrate that the PYR/PYL/RCAR receptors contribute to ROS-mediated activation by ABA of I_{Ca}, thus affecting $[Ca^{2+}]_i$ and its regulation of osmotic solute flux for stomatal closure.

RESULTS

The *pyr1/pyl1/pyl2/pyl4* mutant shows a strong ABA-insensitive phenotype in suppressing stomatal closing and ABA inhibition of stomatal opening (Nishimura et al., 2010; Supplemental Fig. S1). This behavior is consistent with the lower water content and faster water loss we recorded from leaves of the mutant and supports a higher rate of transpiration in the mutant under conditions of drought stress (Supplemental Fig. S2). Despite these characteristics, Nishimura et al. (2010) reported previously that cyclic changes in $[K^+]$ and $[Ca^{2+}]$ outside, manipulations designed to drive $[Ca^{2+}]_i$ oscillations, were sufficient to evoke stomatal closure in the *pyr1/pyl1/pyl2/pyl4* mutant. These findings led us to investigate the Ca^{2+}-sensitive channel activities of the intact guard cells, specifically the response of $I_{K,in}$ and I_{Cl} to ABA.

The *pyr1/pyl1/pyl2/pyl4* Mutant Impairs Inward-Rectifying K^+ and Anion Channel Responses to ABA

We used a two-electrode voltage clamp to record $I_{K,in}$ and I_{Cl} currents during ABA treatments from intact Arabidopsis guard cells (Blatt, 1987; Chen et al., 2012a). Figure 1A shows representative current traces and mean steady-state current-voltage curves for $I_{K,in}$ recorded from wild-type and *pyr1/pyl1/pyl2/pyl4* guard cells. Currents were recorded immediately before and 5 min after adding 20 μM ABA. In the absence of ABA, guard cells of both wild-type and *pyr1/pyl1/pyl2/pyl4* Arabidopsis showed substantial inward currents at voltages negative of −150 mV and current relaxations with half-times of 400 to 600 ms, characteristics typical of the $I_{K,in}$ in Arabidopsis as well as *Vicia* and tobacco (*Nicotiana tabacum*) guard cells (Blatt et al., 1990; Blatt, 1992; Roelfsema and Prins, 1997; Chen et al., 2012a). ABA greatly reduced the amplitude of $I_{K,in}$ in the wild-type guard cells in each of 13 independent experiments, but in guard cells of the *pyr1/pyl1/pyl2/pyl4* mutant, no significant difference in $I_{K,in}$ was observed between measurements before and after adding ABA in any of 10 independent experiments. The average reduction of steady-state $I_{K,in}$ in wild-type guard cells was greater than 90% at all voltages (without ABA, -465 ± 56 $\mu A\ cm^{-2}$; with ABA, -35 ± 4 $\mu A\ cm^{-2}$ at −230 mV); in guard cells of the *pyr1/pyl1/pyl2/pyl4* mutant, the effect of ABA was not significant (without ABA, -542 ± 46 $\mu A\ cm^{-2}$; with ABA, -525 ± 40 $\mu A\ cm^{-2}$ at −230 mV).

We recorded the ensemble anion current, I_{Cl}, from both wild-type and *pyr1/pyl1/pyl2/pyl4* guard cells in separate experiments designed to eliminate the background of K^+ currents (Grabov et al., 1997; Chen et al., 2012a). Figure 1B includes representative current traces and summarizes the mean steady-state I_{Cl} recorded before and after adding 20 μM ABA. Again, in the absence of ABA, both wild-type and mutant guard cells showed current relaxations and steady-state current-voltage relations typical of I_{Cl} when stepped to voltages from +40 to −220 mV (Grabov et al., 1997; Pei et al., 1997; Chen et al., 2012a). In wild-type guard cells, I_{Cl} was enhanced by ABA (without ABA, -229 ± 20 $\mu A\ cm^{-2}$; with ABA, -422 ± 34 $\mu A\ cm^{-2}$ at −160 mV; $n = 15$), but in guard cells of the *pyr1/pyl1/pyl2/pyl4* mutant, the effect of adding ABA was marginal (without ABA, -211 ± 19 $\mu A\ cm^{-2}$; with ABA, -215 ± 24 $\mu A\ cm^{-2}$ at −160 mV; $n = 13$). In short, the responses of both $I_{K,in}$ and I_{Cl} to ABA additions were virtually eliminated in guard cells of the *pyr1/pyl1/pyl2/pyl4* mutant.

ABA-Evoked $[Ca^{2+}]_i$ Increases Are Suppressed in the *pyr1/pyl1/pyl2/pyl4* Mutant

Both $I_{K,in}$ and I_{Cl} represent channel currents sensitive to elevated $[Ca^{2+}]_i$ (Blatt et al., 1990; Grabov and Blatt, 1999; Marten et al., 2007; Chen et al., 2010; Wang et al., 2012), and their loss in responsiveness to ABA in the *pyr1/pyl1/pyl2/pyl4* mutant thus was consistent with a loss in facility for ABA-evoked $[Ca^{2+}]_i$ elevation. To determine if $[Ca^{2+}]_i$ was affected in the mutant, we quantified

Table I. *$I_{K,in}$ gating parameters in response to ABA and external Ca^{2+}*

Nonlinear least-squares fitting of $I_{K,in}$ is from Figures 1 and 4. Data were fitted jointly to a Boltzmann function (Eq. 2) with the gating charge (δ) held in common. Parameters for best fit are indicated for the guard cells of wild-type and *pyr1/pyl1/pyl2/pyl4* mutant Arabidopsis.

Parameter	Wild Type		*pyr1/pyl1/pyl2/pyl4*	
	$-ABA/Ca^{2+}$	$+ABA/Ca^{2+}$	$-ABA/Ca^{2+}$	$+ABA/Ca^{2+}$
ABA				
g_{max} ($\mu S\ cm^2$)	4.8 ± 0.2	0.3 ± 0.1	4.5 ± 0.3	4.4 ± 0.1
$V_{1/2}$ (mV)	−208 ± 2	−236 ± 2	−210 ± 1	−212 ± 4
δ	1.9 ± 0.2			
Ca^{2+}				
g_{max} ($\mu S\ cm^2$)	4.8 ± 0.2	1.6 ± 0.2	4.5 ± 0.3	1.7 ± 0.2
$V_{1/2}$ (mV)	−208 ± 2	−219 ± 2	−210 ± 1	−220 ± 3
δ	1.9 ± 0.2			

$[Ca^{2+}]_i$ by fluorescence ratio imaging after iontophoretic injections of the Ca^{2+}-sensitive dye Fura2. As in the past (Grabov and Blatt, 1998; Köhler and Blatt, 2002; Sokolovski et al., 2008; Wang et al., 2012), fluorescence images were collected at 10-s intervals using a 535-nm interference filter (±20 nm) after excitation with light at 340 and 390 nm, and the fluorescence ratios (f340/f390) were used to quantify $[Ca^{2+}]_i$ during voltage-clamp cycles. Figure 2A includes $[Ca^{2+}]_i$ from wild-type and *pyr1/pyl1/pyl2/pyl4* guard cells determined from fluorescence ratios in the 2-μm band around the cell periphery, a region that typically is subject to Ca^{2+} entry as well as endomembrane Ca^{2+} release (Grabov and Blatt, 1998; Köhler and Blatt, 2002). Figure 2B summarizes the results of all 12 independent experiments before and 5 min after adding 20 μM ABA. ABA evoked significant elevations from resting $[Ca^{2+}]_i$ near 180 nM to a mean value of 487 ± 40 nM in wild-type guard cells. In the absence of ABA, $[Ca^{2+}]_i$ in guard cells of the *pyr1/pyl1/pyl2/pyl4* mutant also situated around 180 nM; ABA treatments of the mutant, however, led to a mean elevation of 259 ± 19 nM, a marginal difference above the mean resting value and not significant at $P < 0.05$. We conclude that guard cells of the *pyr1/pyl1/pyl2/pyl4* mutant are impaired in their ability to raise $[Ca^{2+}]_i$ in response to ABA.

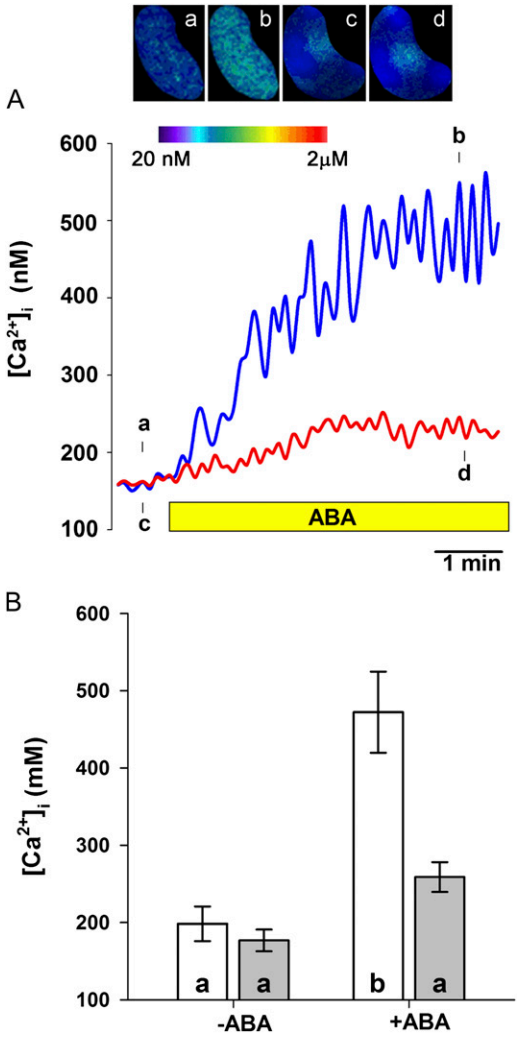

Figure 2. ABA-evoked $[Ca^{2+}]_i$ elevation is suppressed in the *pyr1/pyl1/pyl2/pyl4* mutant. A, Time course of representative Fura2 fluorescence ratio images and peripheral $[Ca^{2+}]_i$ recorded in guard cells of the wild type (a and b; blue line) and the *pyr1/pyl1/pyl2/pyl4* mutant (c and d; red line) before and after adding 20 μM ABA. ABA exposure is indicated below the traces and images cross referenced to time points indicated by lettering. B, $[Ca^{2+}]_i$ before and after ABA in wild-type (white bars; $n = 7$) and *pyr1/pyl1/pyl2/pyl4* mutant (gray bars; $n = 5$) guard cells shown as means ± SE. Significance at $P < 0.02$ is indicated by letters on the bars.

pyr1/pyl1/pyl2/pyl4 Mutant Guard Cells Retain Sensitivity to External Ca^{2+}

Raising the external Ca^{2+} concentration ($[Ca^{2+}]_o$) promotes Ca^{2+} influx through plasma membrane Ca^{2+} channels (Grabov and Blatt, 1998) and has been used to manipulate $[Ca^{2+}]_i$ and stomatal closure in vivo (Allen et al., 2001; Mori et al., 2006; Eisenach et al., 2012). We found previously that $[Ca^{2+}]_o$ inactivates $I_{K,in}$ in Arabidopsis guard cells much as does ABA (Eisenach et al., 2012). To test if these manipulations might bypass the block in elevating $[Ca^{2+}]_i$ in guard cells of the *pyr1/pyl1/pyl2/pyl4* mutant, we compared apertures $I_{K,in}$ and I_{Cl} with guard cells of wild-type Arabidopsis over a range of $[Ca^{2+}]_o$. Figure 3 illustrates the effects of a single step in $[Ca^{2+}]_o$ from 0 to 5 mM over a 30-min period (Fig. 3A), of alternating 5-min steps in $[Ca^{2+}]_o$ between 0 and 10 mM over the same period of time (Fig. 3B), similar to the oscillations in $[Ca^{2+}]_o$ and external K^+ concentrations used to promote so-called "programmed closure" (Allen et al., 2001; Eisenach et al., 2012), and of steady-state apertures recorded after 2 h in $[Ca^{2+}]_o$ from 0 to 10 mM (Fig. 3C). No significant difference was evident between stomata of wild-type and *pyr1/pyl1/pyl2/pyl4* Arabidopsis. In each case, raising $[Ca^{2+}]_o$ was sufficient to suppress stomatal aperture, suggesting that the *pyr1/pyl1/pyl2/pyl4* mutant exhibits a wild-type-like response to $[Ca^{2+}]_o$.

We recorded $I_{K,in}$ and I_{Cl} and their responses to raising $[Ca^{2+}]_o$ from 0.1 to 5 mM in guard cells of both wild-type and *pyr1/pyl1/pyl2/pyl4* mutant Arabidopsis. In each case, raising $[Ca^{2+}]_o$ suppressed $I_{K,in}$ and potentiated I_{Cl}. Mean steady-state current-voltage curves for the two currents are shown in Figure 4, and summaries for the currents recorded at −240 mV ($I_{K,in}$) and −100 mV (I_{Cl}) are included in Figure 5. The results clearly show the substantial effects of raising $[Ca^{2+}]_o$ on the two currents. They also demonstrate the lack of any significant differences in $I_{K,in}$ and I_{Cl} in response to $[Ca^{2+}]_o$ between the wild type and the *pyr1/pyl1/pyl2/pyl4* mutant. Thus, we concluded that a major component of action of the PYR/PYL/RCAR receptor proteins is distinct from the Ca^{2+} sensitivities of the K^+ and anion channels.

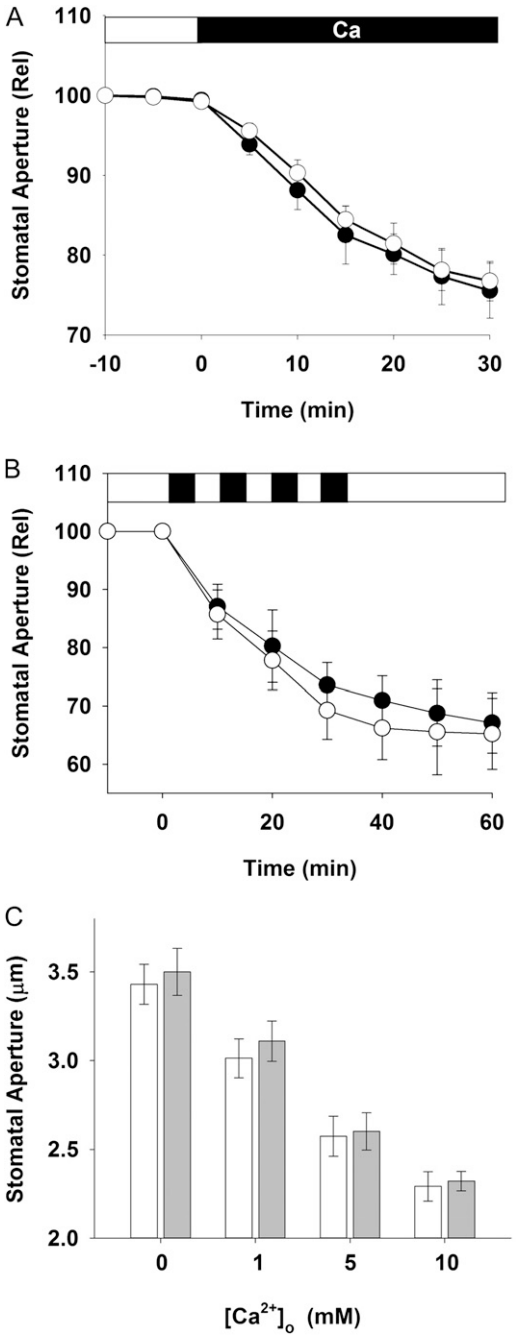

Figure 3. The *pyr1/pyl1/pyl2/pyl4* mutant exhibits a wild-type response to external Ca^{2+}. A, Apertures of stomata from wild-type (white circles) and *pyr1/pyl1/pyl2/pyl4* mutant (black circles) plants in response to a step in $[Ca^{2+}]_o$ from 0.1 to 5 mM in 5 mM MES-KOH, pH 6.1, with 10 mM KCl. Data are means ± SE of five independent experiments (more than 60 stomata) for each line. Apertures were normalized on a cell-by-cell basis to values at a time point 10 min before treatments. B, Apertures of stomata from wild-type (white circles) and *pyr1/pyl1/pyl2/pyl4* mutant (black circles) plants in response to buffer cycling between DB (white bars) and hyperpolarizing buffer (black bars) to drive stomatal closure. Data are means ± SE of four independent experiments (more than 50 stomata) for each line. Apertures were normalized on a cell-by-cell basis to values at a time point 10 min before treatments. C, Absolute steady-state apertures of stomata from wild-type (white bars) and *pyr1/pyl1/pyl2/pyl4* mutant (gray bars) plants in 5 mM MES-KOH, pH 6.1, with Ca^{2+} added as indicated. Data are means ± SE for more than 55 stomata per line at each $[Ca^{2+}]_o$. Differences at any one $[Ca^{2+}]_o$ are not significant at $P < 0.4$.

The *pyr1/pyl1/pyl2/pyl4* Mutant Impairs Ca^{2+} Channel Activation by ABA and ROS

Central to triggering endomembrane Ca^{2+} release and $[Ca^{2+}]_i$ elevation in ABA is a pronounced enhancement of the Ca^{2+} channels at the guard cell plasma membrane (Hamilton et al., 2000), elements of which depend on ABA-induced generation of ROS (Pei et al., 2000). To explore the activity of the Ca^{2+} channels in situ, we took advantage of strategies for isolating the channel currents in these previous studies and our recent finding that the organic acid anion acetate (Ac) suppresses anion channels in the guard cells (Wang and Blatt, 2011). We used two-electrode voltage-clamp methods to measure the Ca^{2+} channel current, I_{Ca}, after first loading the cells with $Ba(Ac)_2$ at pH 7.5, and recordings were carried out in buffer comprising 5 mM MES buffer titrated to pH 6.1 with $Ba(OH)_2$ (final Ba^{2+} concentration, 1 mM). In these circumstances, both K^+ channel currents are blocked by Ba^{2+}, and I_{Cl} was expected to be suppressed by the absence of Cl^- and elevated cytosolic Ac (Wang and Blatt, 2011). Ba^{2+} also permeates the Ca^{2+} channels and, thus, provides the charge carrier for analysis of I_{Ca} (Hamilton et al., 2000, 2001). Figure 6 demonstrates that these methods were sufficient to isolate and resolve I_{Ca} in the intact guard cells. As expected of the Ca^{2+} channels (Hamilton et al., 2000, 2001), the resulting current rectified strongly inward and activated rapidly on negative voltage steps; it showed a reversal voltage close to the expected equilibrium voltage for Ba^{2+} and, in 5 mM Ba^{2+}, was displaced roughly +20 mV, as expected of the Ba^{2+} equilibrium voltage; finally, the current was blocked on adding 1 mM La^{3+} to the bath.

We used this new approach with $Ba(Ac)_2$ to compare I_{Ca} in guard cells of wild-type and *pyr1/pyl1/pyl2/pyl4* Arabidopsis. In both cases, voltage-clamp records yielded similar and appreciable inward-rectifying I_{Ca}, notably at voltages negative from −100 mV. Figure 7 shows that the mean steady-state I_{Ca} values at −200 mV were -235 ± 27 $\mu A\ cm^{-2}$ and -216 ± 21 $\mu A\ cm^{-2}$ for the wild-type ($n = 10$) and *pyr1/pyl1/pyl2/pyl4* ($n = 8$), respectively. Adding ABA, however, uncovered the virtual absence of response in guard cells of the *pyr1/pyl1/pyl2/pyl4* mutant, whereas I_{Ca} in guard cells of wild-type plants rose in amplitude to -462 ± 35 $\mu A\ cm^{-2}$ at a clamp voltage of −200 mV. Thus, the weaker effect on $[Ca^{2+}]_i$ could be ascribed, at least in part, to the failure of ABA to activate plasma membrane Ca^{2+} channels in the *pyr1/pyl1/pyl2/pyl4* mutant.

ABA is known to stimulate ROS synthesis in guard cells, which, in turn, helps activate I_{Ca} (Pei et al., 2000; Kwak et al., 2003). Therefore, we next examined whether ROS production might be suppressed in guard cells of the Arabidopsis *pyr1/pyl1/pyl2/pyl4* mutant. Guard cells were loaded by incubation (Desikan et al., 2004) with

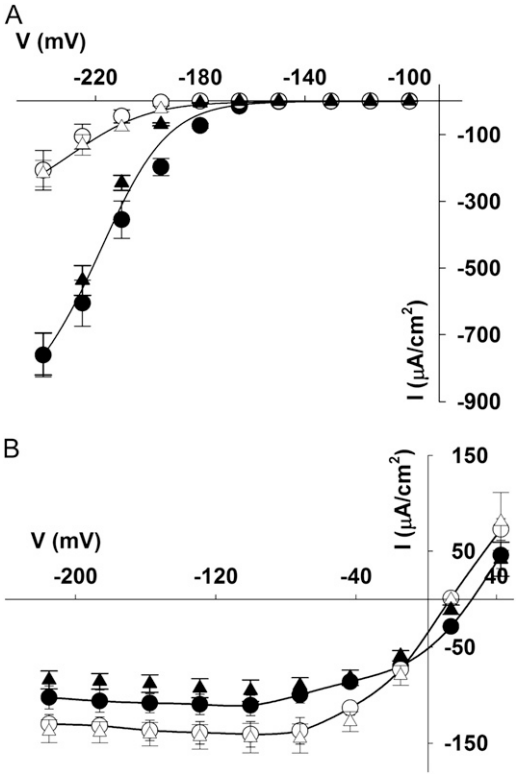

Figure 4. K^+ and Cl^- channel currents of the *pyr1/pyl1/pyl2/pyl4* mutant retain a wild-type response to external Ca^{2+}. A, Steady-state current-voltage curves for $I_{K,in}$ recorded in wild-type (white and black circles; $n = 11$) and *pyr1/pyl1/pyl2/pyl4* mutant (white and black triangles; $n = 9$) guard cells. Data are means ± SE. Black and white symbols denote 1 and 5 mM $[Ca^{2+}]_o$, respectively. Solid curves are fittings to the Boltzmann function (Eq. 2). Parameters are listed in Table I. B, Steady-state current-voltage curves for I_{Cl} recorded in wild-type (white and black circles; $n = 10$) and *pyr1/pyl1/pyl2/pyl4* mutant (white and black triangles; $n = 12$) guard cells. Data are means ± SE. Black and white symbols denote 1 and 5 mM $[Ca^{2+}]_o$, respectively. Solid curves are empirical fittings to third-order polynomials and are included for clarity.

the fluorescent dye 2,7-dichlorofluorescein diacetate (H_2DCFDA), which reports the total ROS activity in the cell (Cárdenas et al., 2006; Stone and Yang, 2006). Figure 8A summarizes the results of four independent experiments and measurements for each line. We found that H_2DCFDA fluorescence increased roughly 1.9-fold after 10 min of treatment of wild-type guard cells with 20 μM ABA. Over the same time period, guard cells of the *pyr1/pyl1/pyl2/pyl4* mutant showed only a 0.9-fold rise in H_2DCFDA fluorescence, indicating that ABA-induced ROS production was reduced in *pyr1/pyl1/pyl2/pyl4*. Parallel experiments (Fig. 8B) showed that stomata of the *pyr1/pyl1/pyl2/pyl4* mutant nonetheless closed in response to exogenous addition of 0.1 mM H_2O_2 much as did stomata of wild-type plants. Finally, we used $Ba(Ac)_2$ loading to examine I_{Ca} following treatment with 0.1 mM H_2O_2. Again, measurements were carried out under voltage clamp before and after adding H_2O_2 to the bath. Figure 8C summarizes the results of 11 independent experiments each with guard cells from wild-type and *pyr1/pyl1/pyl2/pyl4* mutant plants. In both wild-type and *pyr1/pyl1/pyl2/pyl4* guard cells, adding the ROS led to a substantial increase in I_{Ca} at all voltages, the current amplitudes increasing at −200 mV from values near −220 μA cm^{-2} before to values in excess of −600 μA cm^{-2} following H_2O_2 addition. From these observations, we conclude that ABA-evoked I_{Ca} activation is suppressed in the *pyr1/pyl1/pyl2/pyl4* mutant, at least in part as the consequence of reduced ROS production. We return to these points below.

DISCUSSION

Guard cells close the stomatal pore in response to ABA in part by suppressing current through $I_{K,in}$ and activating current through anion channels (I_{Cl}) to depolarize the plasma membrane (Blatt, 2000; Kim et al., 2010). A major driver behind these changes in ion flux is the elevation of $[Ca^{2+}]_i$, which arises from Ca^{2+} entry across the plasma membrane and Ca^{2+}-induced endomembrane Ca^{2+} release. Even so, Ca^{2+}-independent mechanisms are known to regulate $I_{K,in}$ and I_{Cl} in guard cells and have been associated with ABA, including changes in cytosolic pH and protein (de-)phosphorylation. Thus, the recent identification of the PYR/PYL/RCAR or START family of ABA receptor proteins (Park et al., 2009) and their immediate role in regulating protein phosphatase activities has posed questions about the relationship of these events to Ca^{2+}-mediated signaling and its consequences for $I_{K,in}$ and I_{Cl}. In particular,

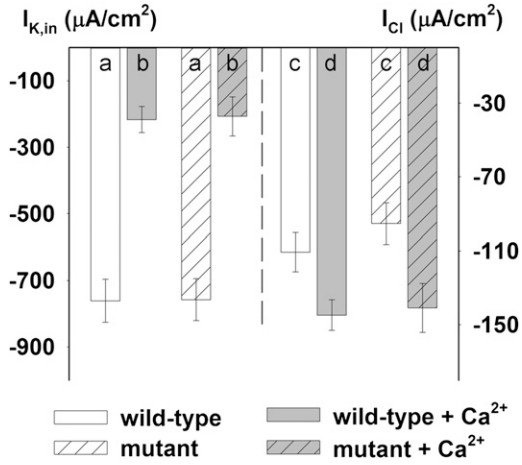

Figure 5. K^+ and Cl^- current amplitudes in the *pyr1/pyl1/pyl2/pyl4* mutant retain a wild-type response to external Ca^{2+}. Inactivation of $I_{K,in}$ and activation of I_{Cl} are seen in response to stepping $[Ca^{2+}]_o$ from 1 to 5 mM. Steady-state currents are from Figure 4, calculated for $I_{K,in}$ at −240 mV and for I_{Cl} at −100 mV in guard cells of wild-type (white bars) and *pyr1/pyl1/pyl2/pyl4* mutant (gray bars) Arabidopsis. Letters in the bars denote significant differences at $P < 0.01$ between the two $[Ca^{2+}]_o$ conditions.

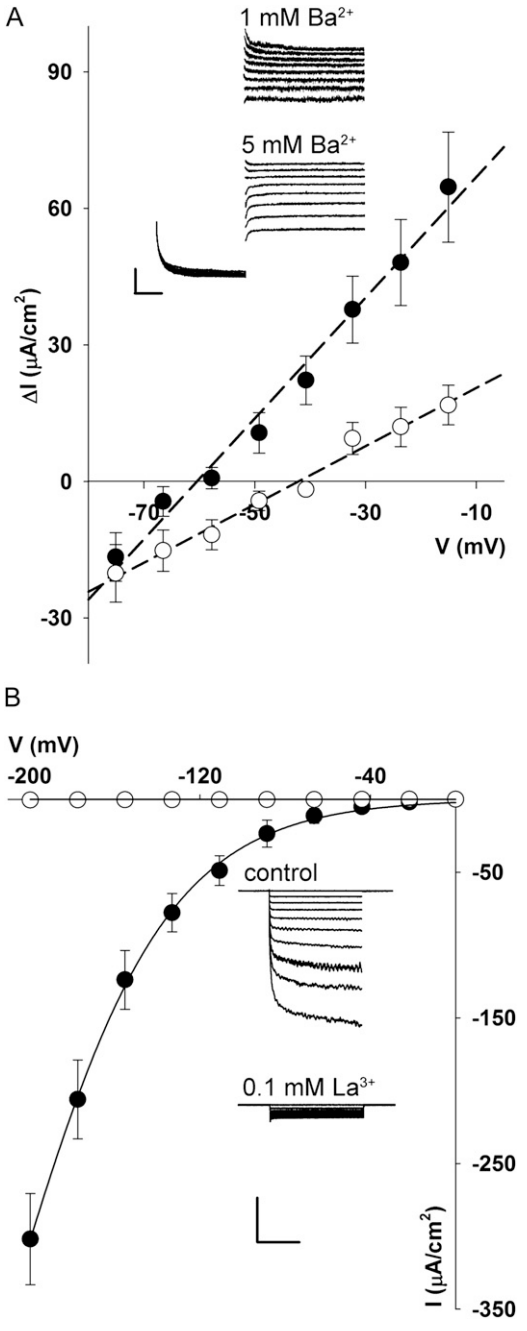

Figure 6. Ion permeation, voltage dependence, and La^{3+} block identify Ca^{2+} channels at the Arabidopsis guard cell plasma membrane. A, Mean of tail current relaxations (Blatt, 2004) after I_{Ca} activation with voltage steps to −200 mV. The analysis shows reversal of the direction of I_{Ca} at −62 ± 4 mV in 1 mM Ba^{2+} (black circles) and −41 ± 4 mV in 5 mM Ba^{2+} (white circles). Data are from eight experiments (guard cells). These values are consistent with the predicted +20-mV shift on raising external [Ba^{2+}] 5-fold and with E_{Ba} of −63 and −43 mV with 150 mM [Ba^{2+}] inside the cell. The inset shows tail currents recorded from one guard cell with 1 and 5 mM Ba^{2+} outside. Scale: vertical, 200 μA cm^{-2}; horizontal, 0.5 s. B, Steady-state current-voltage curves for I_{Ca} recorded in guard cells of wild-type Arabidopsis (n = 11) before (black circles) and after (white circles) adding 1 mM La^{3+} to the bath. Data are means ± SE. Solid curves are empirical polynomial fittings. The inset shows representative I_{Ca} traces during 2-s clamp steps to voltages from 0 to −200 mV. Scale: vertical, 200 μA cm^{-2}; horizontal, 1 s.

direct evidence of a link from the ABA receptors to $[Ca^{2+}]_i$ elevation has been lacking, as has any knowledge of how such connections might be achieved. We have addressed these questions through in vivo measurements of $[Ca^{2+}]_i$ and Ca^{2+} channel currents in parallel with analysis of $I_{K,in}$ and I_{Cl} in the *pyr1/pyl1/pyl2/pyl4* mutant of Arabidopsis. This mutant was previously described to be severely impaired in its capacity to respond to ABA (Nishimura et al., 2010). Our data indicate that the PYR/PYL/RCAR receptor proteins effect a rise in $[Ca^{2+}]_i$ and do so at least in part through changes in Ca^{2+} channel activity at the plasma membrane. Three lines of evidence support this conclusion. (1) Resting $I_{K,in}$ and I_{Cl} activities are retained in guard cells of the Arabidopsis *pyr1/pyl1/pyl2/pyl4* mutant, but the currents do not respond to ABA, nor is $[Ca^{2+}]_i$ elevated in the presence of the hormone. (2) Raising external $[Ca^{2+}]$ is nonetheless sufficient to inactivate $I_{K,in}$, to activate I_{Cl}, and to close the stomata, consistent with a basal I_{Ca} and the increased driving force for Ca^{2+} entry. (3) Direct measurements of I_{Ca} show similar basal Ca^{2+} channel activities in guard cells of wild-type and *pyr1/pyl1/pyl2/pyl4* mutant Arabidopsis, but only in wild-type guard cells is the current enhanced for Ca^{2+} influx following ABA exposure. Finally, we connect the loss in I_{Ca} activation to a reduced level of ROS production in ABA in the *pyr1/pyl1/pyl2/pyl4* mutant. Thus, we are able to build a link between ABA perception and $[Ca^{2+}]_i$ regulation via ROS-mediated activation of Ca^{2+} channels, which, in turn, is sufficient to regulate $I_{K,in}$ and I_{Cl} at the plasma membrane and facilitate stomatal closure.

A Link to $[Ca^{2+}]_i$ Elevation in the *pyr1/pyl1/pyl2/pyl4* Mutant

It has generally been assumed that the failure of stomata to respond to ABA in the *pyr/pyl/rcar* mutants arises from a loss in activation of I_{Cl} and inactivation of $I_{K,in}$ in this mutant (compare Fig. 1 with Supplemental Fig. S1). This connection to the *pyr1/pyl1/pyl2/pyl4* mutant has been ascribed to their regulation primarily by protein (de)phosphorylation. Protein phosphatase and kinase pairs, notably members of the PP2C and SnRK protein families, respectively, have long been known to affect ABA-evoked changes in $I_{K,in}$ and I_{Cl} (Armstrong et al., 1995; Grabov et al., 1997; Pei et al., 1997). Recent studies developed models in vitro around direct interactions between the ABA-related PP2C ABI1, the SnRK OST1, and the dominant guard cell anion channel protein SLAC1 (Geiger et al., 2009a; Umezawa et al., 2009). The KAT1 K^+ channel, which underpins $I_{K,in}$ in Arabidopsis, is also known to interact directly with OST1 (Sato et al., 2009). Thus, the obvious assumption has been that mutations of the ABA receptor complex with ABI1 and its homologs must affect directly, and

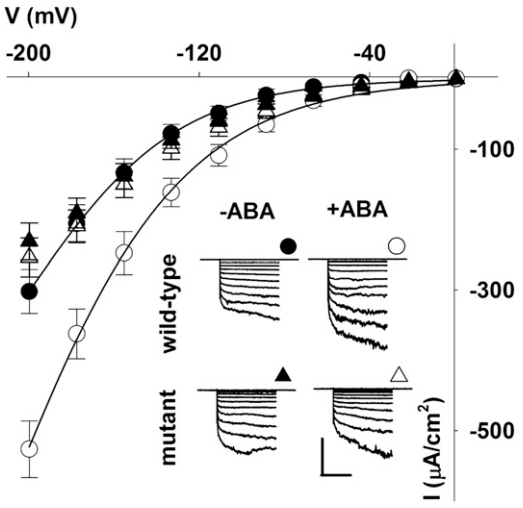

Figure 7. The ABA activation of plasma membrane Ca^{2+} channels is impaired in guard cells of *pyr1/pyl1/pyl2/pyl4* mutant Arabidopsis. Mean steady-state current-voltage curves for I_{Ca} recorded from guard cells of wild-type (white and black circles; $n = 10$) and *pyr1/pyl1/pyl2/pyl4* mutant (white and black triangles; $n = 8$) guard cells are shown. Data are means ± SE. White and black symbols denote without and with 20 μM ABA added, respectively. The inset shows representative I_{Ca} traces during 2-s clamp steps to voltages from 0 to −200 mV cross referenced to the current-voltage curves by symbol. Scale: vertical, 200 μA cm^{-2}; horizontal, 1 s.

first, these downstream targets of the phosphatase-kinase cascade, namely $I_{K,in}$ and I_{Cl}, independent of any effect mediated by $[Ca^{2+}]_i$.

Posited in favor of this argument are observations that external Ca^{2+} affects stomatal aperture, $I_{K,in}$, and I_{Cl} in the *pyr1/pyl1/pyl2/pyl4* mutant, much as it does in guard cells of the wild-type plants (Figs. 3–5; Supplemental Fig. S2). The suggestion is that Ca^{2+} signaling is retained intact in the mutant and, therefore, cannot be responsible for the loss in stomatal response to ABA. The argument does not stand up to closer scrutiny, however. Elevating $[Ca^{2+}]_o$ facilitates Ca^{2+} entry and increases $[Ca^{2+}]_i$ (Grabov and Blatt, 1998; Allen et al., 1999), but it does so by the simple expedient of increasing the driving force and substrate availability for Ca^{2+} influx. True, these findings imply that guard cells of the *pyr1/pyl1/pyl2/pyl4* mutant retain functional Ca^{2+} channels at the plasma membrane and that $I_{K,in}$ and I_{Cl} remain sensitive to $[Ca^{2+}]_i$. However, they tell us nothing of the capacity in the mutant for $[Ca^{2+}]_i$ elevation (i.e. of its regulation), for example, by ABA-enhanced activation of Ca^{2+} channels. For this reason, the data also do not speak to the contribution of $[Ca^{2+}]_i$ to $I_{K,in}$ and I_{Cl} control in the *pyr1/pyl1/pyl2/pyl4* mutant or to its position in any PYR/PYL/RCAR-mediated cascade. Our findings now place the activation of I_{Ca} and its elevation of $[Ca^{2+}]_i$ unequivocally at the center of this cascade. Not only did the *pyr1/pyl1/pyl2/pyl4* mutant suppress $[Ca^{2+}]_i$ increases (Fig. 2) and the response of $I_{K,in}$ and I_{Cl} (Fig. 1) to ABA; we found that the effect on $[Ca^{2+}]_i$ could be traced directly to a loss in response of I_{Ca} to ABA (Fig. 7). These results complement earlier studies indicating that I_{Ca} is activated by ABA and that this effect is membrane delimited (Hamilton et al., 2000), and they also find support in work showing that protein phosphorylation is a prerequisite for the activation of I_{Ca} by ABA (Köhler and Blatt, 2002). This evidence does not preclude other consequences of PYR/PYL/RCAR action, including effects mediated through changes in endomembrane Ca^{2+} release (García-Mata and Lamattina, 2003), but it leaves no doubt of the role of the plasma membrane Ca^{2+} channels, $[Ca^{2+}]_i$, and their importance in PYR/PYL/RCAR-mediated control of the K^+ and Cl^- channels.

Measuring I_{Ca} in Vivo

A key to the success of these studies was our development of a strategy for measuring I_{Ca} in the intact guard cells. Previous work on guard cell Ca^{2+} channels, whether in *Vicia*, tobacco, or Arabidopsis, had relied on patch-clamp recordings from protoplasts (Hamilton et al., 2000; Kwak et al., 2003; Sokolovski et al., 2008). Patch methods ensure access to the cytosol, but they pose a challenge for measurements of channel activities that depend on cytosolic constituents, including soluble proteins and small organic compounds that are dialyzed rapidly against the buffer in the patch pipette. Microelectrode impalements circumvent these difficulties, because the rates of diffusional exchange with the cytosol are generally 10^1- to 10^3-fold lower than those from patch pipettes (Purves, 1981; Blatt and Slayman, 1983; Cannell and Nichols, 1991). Conversely, microelectrode recordings present difficulties when it is desirable to control (in this case, eliminate) permeant anion concentrations inside that contribute substrate for I_{Cl}.

With our discovery that high concentrations of the Ac anion suppress I_{Cl} (Wang and Blatt, 2011), we recognized the potential for eliminating the background of Cl^- channel current, along with those of the K^+ channels, while maintaining current through the Ca^{2+} channels. Our solution was to load the guard cells with $Ba(Ac)_2$ from the microelectrodes while measuring in a Ba^{2+}-containing bath solution. This approach ensured block of the K^+ channels by Ba^{2+} on the two sides of the membrane and of the Cl^- channels by Ac in the cytosol. At the same time, Ba^{2+} provided a charge-carrying ion for permeation of the Ca^{2+} channels, and without Ca^{2+}-mediated suppression of the current in vivo (Hamilton et al., 2000, 2001). Indeed, the currents recorded using this approach show all the hallmarks of I_{Ca} previously described in these earlier patch-clamp studies, including their rapid activation with voltage steps negative going from around −100 mV, their block with millimolar concentrations of lanthanides, and their current reversal at voltages consistent with the Ba^{2+} concentrations on the two sides of the membrane (Figs. 6 and 7). These characteristics indicate that the major current under these conditions is carried by I_{Ca}. We cannot rule out a

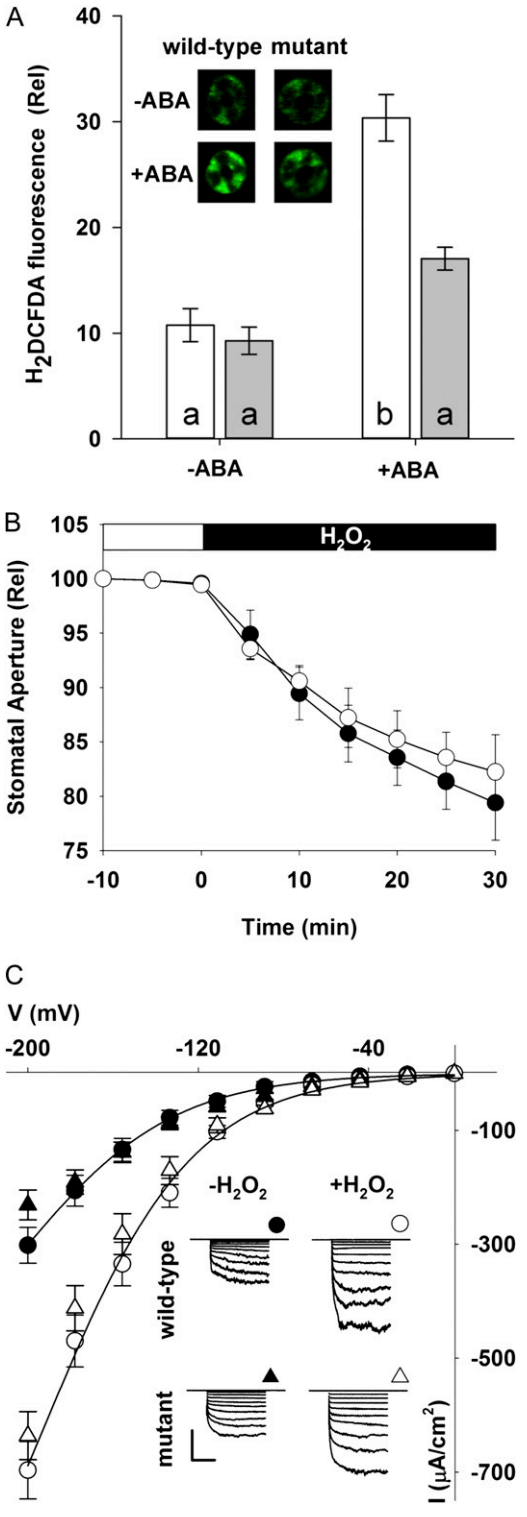

Figure 8. ROS drive stomatal closure and modulate Ca^{2+} channel activity in guard cells of wild-type and *pyr1/pyl1/pyl2/pyl4* mutant Arabidopsis. A, ROS level measured using H_2DCFDA fluorescence in guard cells of the wild-type (white bars) and *pyr1/pyl1/pyl2/pyl4* mutant (gray bars) plants after 30 min either without or with 20 μM ABA. Data are means ± SE ($n = 55$). Significance at $P < 0.01$ is indicated by letters on the bars. The inset shows representative H_2DCFDA fluorescence images of guard cell pairs. B, Stomatal closure induced by adding 100 μM H_2O_2 in wild-type (black circles) and *pyr1/pyl1/pyl2/pyl4* mutant (white circles) guard cells. Apertures were normalized on a cell-by-cell basis to values at a time point 10 min before treatments. Data are means ± SE of $n = 33$ stomata pooled from four independent experiments for each line. C, Mean steady-state current-voltage curves for I_{Ca} recorded in guard cells of wild-type (white and black circles; $n = 11$) and *pyr1/pyl1/pyl2/pyl4* mutant (white and black triangles; $n = 11$) Arabidopsis. Data points are means ± SE. Black and white symbols denote measurements before and 3 min after adding 100 μM H_2O_2 to the bath, respectively. The inset shows representative I_{Ca} traces recorded from wild-type and *pyr1/pyl1/pyl2/pyl4* mutant guard cells before and after H_2O_2 addition. Voltage steps are from 0 to −200 mV. Scale: vertical, 200 μA cm^{-2}; horizontal, 1 s.

small contamination from I_{Cl}, but on the basis of the reversal voltages, we conclude that it must contribute less than 5% to the total current recorded under voltage clamp.

These measurements also permit us to address the question of how many functional Ca^{2+} channels operate at the plasma membrane in the intact guard cell, given our knowledge of the single-channel properties. The ensemble channel current is always related to the single-channel current by the relation

$$I_x = N_x \gamma_x P_o (E_x - V_m) \quad (1)$$

where I is the ensemble current, N is the number of channels, γ_x is the single-channel conductance, P_o is the open probability of the channel, V_m is the membrane potential, and E_x is the equilibrium potential for the permeant ions. If we assume that $P_o = 0.1$ and $\gamma = 13$ pS (Hamilton et al., 2000), then for $I = -800$ pA and $E_x = -40$ mV in 5 mM Ba^{2+} (Fig. 6), we arrive at an estimate for N_x between 1,500 and 2,500 channel units per guard cell, or roughly two to three channels per μm^2. This estimate is within 1 order of magnitude of previous estimates of various channel densities from measurements at the plasma membrane and vacuole of plants (Dietrich et al., 1998; Hafke et al., 2003; Hurst et al., 2004).

Positioning the Ca^{2+} Channels in a PYR/PYL/RCAR Cascade

By their nature in modulating a central subset of protein phosphatases, the PYR/PYL/RCAR receptors are likely to influence a number of target signaling pathways, both directly by affecting the (de)phosphorylation of target proteins and indirectly through their capacity to transmit other signals. As such, resolving the position of the Ca^{2+} channels and $[Ca^{2+}]_i$ elevation in this signaling network is not straightforward. One set of experiments does offer clues to a possible mechanism. We found that ROS production is suppressed to near-background levels in the *pyr1/pyl1/pyl2/pyl4* mutant and that, when exogenously supplied, the ROS H_2O_2 is sufficient to activate the plasma membrane Ca^{2+} channels and potentiate stomatal closure much as

it does in wild-type plants (Fig. 8). These findings accord with earlier evidence that ROS activates I_{Ca} and promotes extracellular Ca^{2+} influx and that ROS production is important for ABA-mediated stomatal response (Pei et al., 2000; Kwak et al., 2003). They indicate that ROS production is one target of the *pyr1/pyl1/pyl2/pyl4* mutation and that this action feeds into the capacity for Ca^{2+} channel activation in the mutant. Again, a parallel can be drawn to mutants that affect protein (de)phosphorylation pathways in the guard cells: the *pyr1/pyl1/pyl2/pyl4* mutation impairs ABA-induced ROS production and stomatal closure, as do the ABA-insensitive *abi1-1* and *ost1* mutations (Murata et al., 2001). We can make a connection now also to activation of the plasma membrane Ca^{2+} channels through ROS production.

In conclusion, we have identified a role for plasma membrane Ca^{2+} channels and $[Ca^{2+}]_i$ elevation in the PYR/PYL/RCAR receptor-mediated response of stomatal guard cells to ABA. A key to these studies was the development of methods for recording Ca^{2+} channel current and $[Ca^{2+}]_i$ as well as K^+ and Cl^- currents in the intact guard cells of Arabidopsis, both in the wild type and the *pyr1/pyl1/pyl2/pyl4* mutant. The observations do not rule out other effects mediated by PYR/PYL/RCAR (de)phosphorylation cascades (indeed, these are to be expected), but they argue strongly for the central role of $[Ca^{2+}]_i$ elevation underlying their capacity to drive ABA-induced stomatal closure. Thus, our findings underline the importance of Ca^{2+} channel activation as an early step in the connection between ABA binding to the PYR/PYL/RCAR proteins and their subsequent regulation of K^+ and Cl^- channels, including KAT1 and SLAC1, at the guard cell plasma membrane.

MATERIALS AND METHODS

Plant Growth and Preparation

Wild-type Arabidopsis (*Arabidopsis thaliana* ecotype Columbia) and the *pyr1/pyl1/pyl2/pyl4* quadruple mutant in the same background, obtained from Sean Cutler, were sown in compost and grown under a 8-h/16-h day/night cycle (100 μmol m^{-2} s^{-1}) and 60% humidity in the growth chambers (Sanyo). Leaves were harvested for experiments from plants after 4 to 6 weeks of growth.

Stomatal Apertures

Stomatal apertures were measured in epidermal peels of newly expanded leaves. Peels were taken from the abaxial leaf surface and were fixed to the glass bottom of the experimental chamber after coating the chamber surface with an optically clear and pressure-sensitive silicone adhesive. All operations were carried out on an Axiovert 200 (Zeiss) fitted with Nomarski differential interference contrast optics and 40× LD Achroplan objective. Peels were bathed in continuous flowing solution fed at a rate of 10 chamber volumes min^{-1}. The standard perfusion medium (SB) contained 10 mM KCl and 5 mM MES titrated with $Ca(OH)_2$ to its pK_a at 6.1 (1 mM $[Ca^{2+}]$). In experiments with ABA, Ca^{2+}, and H_2O_2 treatments, peels were preincubated in depolarizing buffer (DB; 5 mM MES-KOH, pH 6.1, and 60 mM KCl) for 2 h under 150 μmol m^{-2} s^{-1} photosynthetically active radiation to open stomata. To evoke closure by $[Ca^{2+}]_o$ elevation, the tissue was superfused by exchange of DB with hyperpolarizing buffer [HB = 5 mM MES-$Ca(OH)_2$, pH 6.1, 0.1 mM KCl, and 5 mM $CaCl_2$] at 5-min intervals (Eisenach et al., 2012). In experiments testing the effects of $[Ca^{2+}]_o$, peels were bathed in 5 mM MES-KOH, pH 6.1, with 10 mM KCl and $[Ca^{2+}]$ as indicated added as $CaCl_2$. Measurements were taken at 5-min intervals using an AxioCam HD digital camera and AxioVision software (Zeiss). Stomatal apertures were determined offline after calibration using ImageJ version 1.43 (www.rsb.info.nih.gov/ij/).

Electrophysiology

Electrical recordings were carried out using double- and triple-barreled microelectrodes essentially as described before (Blatt and Armstrong, 1993; Garcia-Mata et al., 2003; Chen et al., 2012a). For measurements of K^+ currents, microelectrode barrels were filled with 200 mM K-Ac, pH 7.5, to avoid Cl^- loading and interference of anion currents. For measurements of anion currents, both electrode barrels were filled with 300 mM CsCl, pH 7.5, and the tissue was superfused with 5 mM MES-$Ca(OH)_2$, pH 6.1, containing 15 mM CsCl and 15 mM tetraethylammonium chloride. For measurements of Ca^{2+} channel current, electrode barrels were filled with 150 mM $Ba(Ac)_2$, pH 7.5, and the tissue was superfused with buffer containing 5 mM MES titrated to pH 6.1 with $Ba(OH)_2$ (1 mM $[Ba^{2+}]$). Additional Ba^{2+} was added as $BaCl_2$. Membrane voltage was brought under experimental control by standard, two-electrode voltage clamp (Blatt and Armstrong, 1993; Blatt, 2004) using Henry's EP software (Y-Science, University of Glasgow; Hills and Volkov, 2004). Surface areas and volumes of impaled guard cells were calculated assuming a spheroid geometry (Blatt and Armstrong, 1993).

Current kinetics and current-voltage analyses were carried out using Henry's EP software as described previously (Blatt, 2004; Hills and Volkov, 2004; Chen et al., 2012a). Nonlinear least-squares fittings were carried using a Boltzmann function of the form

$$I = \frac{g_{max}(V - E_K)}{1 + e^{\delta zF(V - V_{1/2})/RT}} \quad (2)$$

where δ is the voltage sensitivity coefficient (gating charge), E_K is the K^+ equilibrium voltage, g_{max} is the maximum conductance of the ensemble of channels, $V_{1/2}$ is the voltage yielding half-maximal activation, and F is the Faraday constant, R is the universal gas constant, and T is the absolute temperature.

$[Ca^{2+}]_i$ Measurements

$[Ca^{2+}]_i$ was determined by Fura2 fluorescence ratio imaging using a cooled Pentamax-512 CCD camera and GenIV intensifier (Princeton Instruments) as described previously (Köhler and Blatt, 2002; Garcia-Mata et al., 2003). Dye was loaded by iontophoresis using three-barreled microelectrodes, the third barrel filled with 0.1 mM Fura2 as the free acid, while clamping the membrane voltage to −50 mV. Fluorescence image pairs were collected at 2-, 5-, and 10-s intervals using a 535-nm interference filter (±20 nm bandwidth) after exciting with 340- and 390-nm light (10-nm slit width; Polychrom II; Til Photonics). Images were corrected for background fluorescence recorded before dye loading, and fluorescence and fluorescence ratios were analyzed using MetaFluor and MetaMorph software version 6.1 (Universal Imaging). Dye loading was judged successful by visual checks for cytosolic dye distribution and by stabilization of the fluorescence ratio signal. Fura2 fluorescence was calibrated as before (Grabov and Blatt, 1998; Köhler and Blatt, 2002). Estimates of dye loading indicated final Fura2 concentrations of 2 to 10 μM.

ROS

Production of ROS was monitored using the ROS-sensitive fluorescent probe H_2DCFDA (Invitrogen) using the method described by Desikan et al. (2004). Epidermal peels were pretreated with DB in the light for 2 h before loading by superfusion with 15 μM H_2DCFDA in the same buffer for 20 min in the dark. Thereafter, peels were superfused with SB to remove excess dye. Peels were incubated in SB without and with 20 μM ABA for 30 min, and H_2DCFDA fluorescence was monitored at 10-min intervals using a Zeiss LSM 510 META confocal microscope fitted with 40× and 63× Achroplan oil-immersion objectives (Zeiss). H_2DCFDA was excited using the 488-nm line from an argon laser, and fluorescence emission was collected after passage through a 505- to 550-nm bandpass filter and was corrected for background fluorescence recorded prior to H_2DCFDA loading.

Data Analysis

Current-voltage curves and statistical analyses were carried out using SigmaPlot 11 (Systat Software; http://www.sigmaplot.com). Nonlinear least-squares fittings used a Marquardt-Levenberg algorithm (Marquardt, 1963). Significance was tested using Student's *t* test and ANOVA. Otherwise, data are reported as means ± SE of *n* observations.

Supplemental Data

The following materials are available in the online version of this article.

Supplemental Figure S1. The *pyr1/pyl1/pyl2/pyl4* mutant suppresses ABA-evoked stomatal closure.

Supplemental Figure S2. The *pyr1/pyl1/pyl2/pyl4* mutant shows enhanced water loss.

ACKNOWLEDGMENTS

We thank Sean Cutler (University of California, Riverside) for seed of the *pyr1/pyl1/pyl2/pyl4* mutant and Christopher Grefen and Anna Amtmann (University of Glasgow) for comments during the preparation of the manuscript.

Received April 17, 2013; accepted July 25, 2013; published July 30, 2013.

LITERATURE CITED

Allen GJ, Chu SP, Harrington CL, Schumacher K, Hoffmann T, Tang YY, Grill E, Schroeder JI (2001) A defined range of guard cell calcium oscillation parameters encodes stomatal movements. Nature **411:** 1053–1057

Allen GJ, Kuchitsu K, Chu SP, Murata Y, Schroeder JI (1999) *Arabidopsis abi1-1* and *abi2-1* phosphatase mutations reduce abscisic acid-induced cytoplasmic calcium rises in guard cells. Plant Cell **11:** 1785–1798

Armstrong F, Leung J, Grabov A, Brearley J, Giraudat J, Blatt MR (1995) Sensitivity to abscisic acid of guard-cell K^+ channels is suppressed by *abi1-1*, a mutant *Arabidopsis* gene encoding a putative protein phosphatase. Proc Natl Acad Sci USA **92:** 9520–9524

Blatt MR (1987) Electrical characteristics of stomatal guard cells: the contribution of ATP-dependent, "electrogenic" transport revealed by current-voltage and difference-current-voltage analysis. J Membr Biol **98:** 257–274

Blatt MR (1992) K^+ channels of stomatal guard cells: characteristics of the inward rectifier and its control by pH. J Gen Physiol **99:** 615–644

Blatt MR (2000) Cellular signaling and volume control in stomatal movements in plants. Annu Rev Cell Dev Biol **16:** 221–241

Blatt MR (2004) Concepts and techniques in plant membrane physiology. *In* MR Blatt, ed, Membrane Transport in Plants, Vol 15. Blackwell, Oxford, pp 1–39

Blatt MR, Armstrong F (1993) K^+ channels of stomatal guard cells: abscisic acid-evoked control of the outward rectifier mediated by cytoplasmic pH. Planta **191:** 330–341

Blatt MR, Slayman CL (1983) KCl leakage from microelectrodes and its impact on the membrane parameters of a nonexcitable cell. J Membr Biol **72:** 223–234

Blatt MR, Thiel G, Trentham DR (1990) Reversible inactivation of K^+ channels of *Vicia* stomatal guard cells following the photolysis of caged inositol 1,4,5-trisphosphate. Nature **346:** 766–769

Cannell MB, Nichols CG (1991) Effects of pipette geometry on the time course of solution change in patch clamp experiments. Biophys J **60:** 1156–1163

Cárdenas L, McKenna ST, Kunkel JG, Hepler PK (2006) NAD(P)H oscillates in pollen tubes and is correlated with tip growth. Plant Physiol **142:** 1460–1468

Chen ZH, Eisenach C, Xu XQ, Hills A, Blatt MR (2012a) Protocol: optimised electrophyiological analysis of intact guard cells from Arabidopsis. Plant Methods **8:** 15–25

Chen ZH, Hills A, Bätz U, Amtmann A, Lew VL, Blatt MR (2012b) Systems dynamic modeling of the stomatal guard cell predicts emergent behaviors in transport, signaling, and volume control. Plant Physiol **159:** 1235–1251

Chen ZH, Hills A, Lim CK, Blatt MR (2010) Dynamic regulation of guard cell anion channels by cytosolic free Ca^{2+} concentration and protein phosphorylation. Plant J **61:** 816–825

Desikan R, Cheung MK, Bright J, Henson D, Hancock JT, Neill SJ (2004) ABA, hydrogen peroxide and nitric oxide signalling in stomatal guard cells. J Exp Bot **55:** 205–212

Dietrich P, Dreyer I, Wiesner P, Hedrich R (1998) Cation sensitivity and kinetics of guard-cell potassium channels differ among species. Planta **205:** 277–287

Eisenach C, Chen ZH, Grefen C, Blatt MR (2012) The trafficking protein SYP121 of Arabidopsis connects programmed stomatal closure and K^+ channel activity with vegetative growth. Plant J **69:** 241–251

Garcia-Mata C, Gay R, Sokolovski S, Hills A, Lamattina L, Blatt MR (2003) Nitric oxide regulates K^+ and Cl^- channels in guard cells through a subset of abscisic acid-evoked signaling pathways. Proc Natl Acad Sci USA **100:** 11116–11121

García-Mata C, Lamattina L (2003) Abscisic acid, nitric oxide and stomatal closure: is nitrate reductase one of the missing links? Trends Plant Sci **8:** 20–26

Geiger D, Becker D, Vosloh D, Gambale F, Palme K, Rehers M, Anschuetz U, Dreyer I, Kudla J, Hedrich R (2009a) Heteromeric AtKC1·AKT1 channels in Arabidopsis roots facilitate growth under K^+-limiting conditions. J Biol Chem **284:** 21288–21295

Geiger D, Scherzer S, Mumm P, Stange A, Marten I, Bauer H, Ache P, Matschi S, Liese A, Al-Rasheid KAS, et al (2009b) Activity of guard cell anion channel SLAC1 is controlled by drought-stress signaling kinase-phosphatase pair. Proc Natl Acad Sci USA **106:** 21425–21430

Grabov A, Blatt MR (1998) Membrane voltage initiates Ca^{2+} waves and potentiates Ca^{2+} increases with abscisic acid in stomatal guard cells. Proc Natl Acad Sci USA **95:** 4778–4783

Grabov A, Blatt MR (1999) A steep dependence of inward-rectifying potassium channels on cytosolic free calcium concentration increase evoked by hyperpolarization in guard cells. Plant Physiol **119:** 277–288

Grabov A, Leung J, Giraudat J, Blatt MR (1997) Alteration of anion channel kinetics in wild-type and *abi1-1* transgenic *Nicotiana benthamiana* guard cells by abscisic acid. Plant J **12:** 203–213

Hafke JB, Hafke Y, Smith JAC, Lüttge U, Thiel G (2003) Vacuolar malate uptake is mediated by an anion-selective inward rectifier. Plant J **35:** 116–128

Hamilton DWA, Hills A, Blatt MR (2001) Extracellular Ba^{2+} and voltage interact to gate Ca^{2+} channels at the plasma membrane of stomatal guard cells. FEBS Lett **491:** 99–103

Hamilton DWA, Hills A, Kohler B, Blatt MR (2000) Ca^{2+} channels at the plasma membrane of stomatal guard cells are activated by hyperpolarization and abscisic acid. Proc Natl Acad Sci USA **97:** 4967–4972

Hills A, Chen ZH, Amtmann A, Blatt MR, Lew VL (2012) OnGuard, a computational platform for quantitative kinetic modeling of guard cell physiology. Plant Physiol **159:** 1026–1042

Hills A, Volkov V (2004) Electrophysiology equipment and software. *In* MR Blatt, ed, Membrane Transport in Plants, Vol 15. Blackwell, Oxford, pp 40–71

Hurst AC, Meckel T, Tayefeh S, Thiel G, Homann U (2004) Trafficking of the plant potassium inward rectifier KAT1 in guard cell protoplasts of *Vicia faba*. Plant J **37:** 391–397

Keller BU, Hedrich R, Raschke K (1989) Voltage-dependent anion channels in the plasma membrane of guard cells. Nature **341:** 450–453

Kim TH, Böhmer M, Hu HH, Nishimura N, Schroeder JI (2010) Guard cell signal transduction network: advances in understanding abscisic acid, CO_2, and Ca^{2+} signaling. Annu Rev Plant Biol **61:** 561–591

Köhler B, Blatt MR (2002) Protein phosphorylation activates the guard cell Ca^{2+} channel and is a prerequisite for gating by abscisic acid. Plant J **32:** 185–194

Kwak JM, Mori IC, Pei ZM, Leonhardt N, Torres MA, Dangl JL, Bloom RE, Bodde S, Jones JDG, Schroeder JI (2003) NADPH oxidase AtrbohD and AtrbohF genes function in ROS-dependent ABA signaling in *Arabidopsis*. EMBO J **22:** 2623–2633

Leckie CP, McAinsh MR, Allen GJ, Sanders D, Hetherington AM (1998) Abscisic acid-induced stomatal closure mediated by cyclic ADP-ribose. Proc Natl Acad Sci USA **95:** 15837–15842

Lemtiri-Chlieh F, MacRobbie EAC (1994) Role of calcium in the modulation of *Vicia* guard cell potassium channels by abscisic acid: a patch-clamp study. J Membr Biol **137:** 99–107

Li JX, Assmann SM (1996) An abscisic acid-activated and calcium-independent protein kinase from guard cells of fava bean. Plant Cell **8:** 2359–2368

Marquardt D (1963) An algorithm for least-squares estimation of nonlinear parameters. J Soc Ind Appl Math **11:** 431–441

Marten H, Konrad KR, Dietrich P, Roelfsema MRG, Hedrich R (2007) Ca^{2+}-dependent and -independent abscisic acid activation of plasma membrane anion channels in guard cells of *Nicotiana tabacum*. Plant Physiol **143:** 28–37

McAinsh MR, Brownlee C, Hetherington AM (1990) Abscisic acid-induced elevation of guard cell cytosolic Ca^{2+} precedes stomatal closure. Nature **343:** 186–188

Mori IC, Murata Y, Yang YZ, Munemasa S, Wang YF, Andreoli S, Tiriac H, Alonso JM, Harper JF, Ecker JR, et al (2006) CDPKs CPK6 and CPK3 function in ABA regulation of guard cell S-type anion- and Ca^{2+}-permeable channels and stomatal closure. PLoS Biol **4:** 1749–1762

Murata Y, Pei ZM, Mori IC, Schroeder J (2001) Abscisic acid activation of plasma membrane Ca^{2+} channels in guard cells requires cytosolic NAD(P)H and is differentially disrupted upstream and downstream of reactive oxygen species production in *abi1-1* and *abi2-1* protein phosphatase 2C mutants. Plant Cell **13:** 2513–2523

Mustilli AC, Merlot S, Vavasseur A, Fenzi F, Giraudat J (2002) *Arabidopsis* OST1 protein kinase mediates the regulation of stomatal aperture by abscisic acid and acts upstream of reactive oxygen species production. Plant Cell **14:** 3089–3099

Neill SJ, Desikan R, Clarke A, Hancock JT (2002) Nitric oxide is a novel component of abscisic acid signaling in stomatal guard cells. Plant Physiol **128:** 13–16

Nishimura N, Sarkeshik A, Nito K, Park SY, Wang A, Carvalho PC, Lee S, Caddell DF, Cutler SR, Chory J, et al (2010) *PYR/PYL/RCAR* family members are major in-vivo ABI1 protein phosphatase 2C-interacting proteins in *Arabidopsis*. Plant J **61:** 290–299

Park SY, Fung P, Nishimura N, Jensen DR, Fujii H, Zhao Y, Lumba S, Santiago J, Rodrigues A, Chow TFF, et al (2009) Abscisic acid inhibits type 2C protein phosphatases via the *PYR/PYL* family of START proteins. Science **324:** 1068–1071

Pei ZM, Kuchitsu K, Ward JM, Schwarz M, Schroeder JI (1997) Differential abscisic acid regulation of guard cell slow anion channels in *Arabidopsis* wild-type and *abi1* and *abi2* mutants. Plant Cell **9:** 409–423

Pei ZM, Murata Y, Benning G, Thomine S, Klüsener B, Allen GJ, Grill E, Schroeder JI (2000) Calcium channels activated by hydrogen peroxide mediate abscisic acid signalling in guard cells. Nature **406:** 731–734

Purves JD (1981) Microelectrode Methods for Intracellular Recording and Ionophoresis. Academic Press, London

Roelfsema MRG, Prins HBA (1997) Ion channels in guard cells of *Arabidopsis thaliana* (L.) Heynh. Planta **202:** 18–27

Sato A, Sato Y, Fukao Y, Fujiwara M, Umezawa T, Shinozaki K, Hibi T, Taniguchi M, Miyake H, Goto DB, et al (2009) Threonine at position 306 of the KAT1 potassium channel is essential for channel activity and is a target site for ABA-activated SnRK2/OST1/SnRK2.6 protein kinase. Biochem J **424:** 439–448

Sokolovski S, Hills A, Gay R, Garcia-Mata C, Lamattina L, Blatt MR (2005) Protein phosphorylation is a prerequisite for intracellular Ca^{2+} release and ion channel control by nitric oxide and abscisic acid in guard cells. Plant J **43:** 520–529

Sokolovski S, Hills A, Gay RA, Blatt MR (2008) Functional interaction of the SNARE protein NtSyp121 in Ca^{2+} channel gating, Ca^{2+} transients and ABA signalling of stomatal guard cells. Mol Plant **1:** 347–358

Stone JR, Yang SP (2006) Hydrogen peroxide: a signaling messenger. Antioxid Redox Signal **8:** 243–270

Thiel G, MacRobbie EAC, Blatt MR (1992) Membrane transport in stomatal guard cells: the importance of voltage control. J Membr Biol **126:** 1–18

Umezawa T, Sugiyama N, Mizoguchi M, Hayashi S, Myouga F, Yamaguchi-Shinozaki K, Ishihama Y, Hirayama T, Shinozaki K (2009) Type 2C protein phosphatases directly regulate abscisic acid-activated protein kinases in Arabidopsis. Proc Natl Acad Sci USA **106:** 17588–17593

Wang Y, Blatt MR (2011) Anion channel sensitivity to cytosolic organic acids implicates a central role for oxaloacetate in integrating ion flux with metabolism in stomatal guard cells. Biochem J **439:** 161–170

Wang Y, Papanatsiou M, Eisenach C, Karnik R, Williams M, Hills A, Lew VL, Blatt MR (2012) Systems dynamic modeling of a guard cell Cl^- channel mutant uncovers an emergent homeostatic network regulating stomatal transpiration. Plant Physiol **160:** 1956–1967